An accelerated decarbonylation of 5-hydroxymethylfurfural in compressed carbon dioxide: a facile approach

Journal:	*Green Chemistry*
Manuscript ID	GC-ART-01-2018-000174.R3
Article Type:	Paper
Date Submitted by the Author:	06-Apr-2018
Complete List of Authors:	Chatterjee, Maya; National Institute of Advanced Industrial Science and Technology, Supercritical Fluid Research Center Ishizaka, Takayuki; National Institute of Advanced Science and Technology, Research Center for Compact Chemical Process Kawanami, Hajime; National Institute of Advanced Science and Technology, Research Institute for Chemical Process Technology

SCHOLARONE™
Manuscripts

An accelerated decarbonylation of 5-hydroxymethylfurfural in compressed carbon dioxide: a facile approach

Maya Chatterjee*[a], Takayuki Ishizaka [a] and Hajime Kawanami* [a, b]

[a] *Microflow Chemistry Group, Research Institute for Chemical Process Technology AIST Tohoku, 4-2-1, Nigatake, Miyagino-ku, Sendai, 983-8551, Japan, Tel: 81 22 237 5213; Fax: 81 22 237 5388*

[b] *CREST, Japan Science and Technology (JST), 4-1-8, Honcho, Kawaguchi, Saitama,332-0012, Japan*

Abstract

The decarbonylation of biomass-based 5-hydroxymethylfurfural (HMF) in compressed CO_2 features an unexpected acceleration of the reaction rate with excellent catalytic activity is reported. Without any additive, CO surrogates or any organic solvents, the developed method afforded an excellent conversion (99.8%) and highest selectivity of furfuryl alcohol (99.6%) in 4h at 145 °C using alumina supported Pd catalyst (Pd/Al_2O_3). The superior activity rely on the unique characteristics (miscibility of reactant gases and high diffusivity) of compressed CO_2 and synergy between CO_2 and Pd/Al_2O_3, where CO_2 played an interesting role to accelerate the reaction through the enhanced diffusion of CO and furfuryl alcohol (both of the products have large solubility in CO_2), consequently shifted the equilibrium to the forward direction. Characterisation of the catalyst suggested a direct interaction with the substrate, and provides an indication of the possible reaction path, thus a mechanism would be outlined. Compare to the results reported in organic solvents, compressed CO_2 overpowers in terms of activity, selectivity and reaction rate. This strategy

highlights easy product separation, improved catalyst life and a simple sustainable process. The efficiency of this protocol is confirmed from its potential application on a series of aldehydes with various substituent to produce decarbonylated product with good to excellent yield.

Introduction

Biomass represents a vast renewable resource suitable as a potential replacement of fossil fuel for the development of a sustainable society. Naturally produced lignocellulosic biomass (a dry plant based material) with intricate polymeric structure consisted of various oxygenated functionalities. One of the targeted strategies of the implementation of bio-feedstock is the upgradation through the reduction of oxygen content using defunctionalisation processes, which includes hydrogenation, dehydration and hydrodeoxygenation. In addition, decarbonylation, although, represents an effective way of transformation, but currently a less-studied process considering the biomass derived compounds. As a major step towards the development of effective catalysts, the metal based homogeneous systems with different ligands, use of CO scavengers for improved activity as well as acceptor-less conditions[1-3] were investigated. The drawbacks associated with the developed catalytic systems are mainly related to the recovery of catalysts after the reaction, harsh reaction conditions together with the requirement of high-boiling solvents make the decarbonylation process incompatible with the sustainable reaction procedure.

In this context, heterogeneous catalysts would be of great interest compared to the homogeneous system because it provides a straightforward manner of catalyst/product separation through filtration, thus, makes the catalyst recovery easier, however, with lower reaction rate. Hence, earlier reports on the selective decarbonylation of different aromatic aldehydes using heterogeneous catalysts associated with the gas phase reaction, which faced the difficulties of tedious reaction conditions, presence of additives, catalytic deactivation and low product yield.[4] In the following years, search was continued for the

development of a suitable decarbonylation catalysts to perform under milder reaction conditions in different organic solvents using metal nanoparticles or supported metal nanoparticles as catalysts [5] but with the limitations such as requirement of metal additive, CO scavenger, use of large excess of organic solvents, longer reaction time and also the product separation.

Furan-based compounds proves versatility in the generation of variety of products, reveals the potential implementations into the bio-refinery concept, thus, several strategy was developed for their transformations to different speciality chemicals. Being a multifunctional compound, 5-hydroxymethylfurfural (HMF), provides a beneficial feature to the production of a wide spectrum of materials related to fuel or non-fuel category through hydrogenation, oxidation, hydrogenolysis of C-O bond, dehydrogenation, decarbonylation, rearrangement, dissociation and polymerisation.[6]

Deacarbonylation of the –CHO group, requires an abstraction of aldehydic hydrogen, which is an endothermic reaction, thus, elevated temperature is essential for this process. In this context, one of the main challenges is to avoid the humin formation (soluble or insoluble polymeric species), generally occurs at higher temperature and hampers catalytic activity.[7] In addition, presence of the highly active multi-functional groups result different side reactions and consequently decreased the selectivity of decarbonylated product. Additionally, adsorption and desorption of CO causes deactivation to the metal surface. Rauchfuss and co-workers employed an open system using Pd/C catalyst at comparatively lower temperature (120 °C), but presence of oxygen might be inappropriate for the reduced catalysts as well as for highly active HMF.[8] A heterogeneous Pd catalysts supported on

mesoporous silica (SBA-15) produces promising results in cyclohexane,[9] however, necessitate the presence of molecular sieve (MS 4A) as CO surrogates (negative consequence is the regeneration of MS 4A, which is a tedious process and changed the resin composition), prolonged reaction time (12h), restricted substrate scope and recyclability. To improve the yield, Meng *et al.* applied alkali metal modified Pd catalysts; the decarbonylated product obtained at 180 °C with the yield of >90% in 16h of reaction, after purging N_2 at 8h interval to prevent deactivation.[10a] The same group also employed 28% water along with 1-4-dioxane and improve the yield of furfuryl alcohol (95.3%) under the same conditions as their previous report, but in hydrogen atmosphere; flushing fresh hydrogen after 8h.[10b] The use of hydrogen as a carrier gas require an explanation to distinguish between hydrogenation and decarbonylation as furfural moiety can be readily hydrogenated on Pd catalyst, which is missing in the report. Despite advances in the decarbonylation reaction using heterogeneous catalysts, still has limited success, because of the requirement of harsh reaction conditions, longer reaction time as well as the use of CO acceptor.

Compressed carbon dioxide (compressed CO_2) is a promising alternative for rapid and selective organic synthesis related to its unique properties such as enhanced diffusion rates, easy product separation, controls mass transfer resistance and improvement of catalyst lifetime. However, reactions with heterogeneous catalysts are still restricted mainly to hydrogenation and oxidation because of accelerated reaction rates and different product distributions, as well as high selectivity, associated to the miscibility of the reactant gases (H_2 and O_2). A combination of heterogeneous catalysts and compressed CO_2, can provide

an immense opportunity to develop highly efficient, environmentally and economically beneficial processes, hence, can be a sustainable extension to the organic synthesis. Geilen *et al.* first reported the decarbonylation of HMF using a homogeneous Ir catalyst ([IrCl (cod)]$_2$) with different phosphine ligands in 1,4-dioxane along with 5 MPa of compressed CO_2. Although, HMF was decarbonylated to furfuryl alcohol with 95% selectivity, require dioxane as a solvent, very high temperature (220 °C) and long reaction time (12h).[11]

In our previous work, we have successfully developed a strategy to dehydrogenate alcohol over heterogeneous Rh catalyst in compressed CO_2 using HMF as a model compound.[12] During dehydrogenation, decarbonylation of the aldehyde group was detected as a competitor reaction to produce furfuryl alcohol depending on the reaction conditions. While screening the different metal catalysts for dehydrogenation, we observed that Pd has the ability to mediate both the reactions (dehydrogenation of alcohols and decarbonylation of aldehyde) in one transformation, but, tuning of reaction parameters can dictate the reaction in a desired direction.

Here, we attempted the decarbonylation of HMF using a commercially available Pd/Al_2O_3 catalysts, focusing on the use of only compressed CO_2 to play the dual role as a solvent and surrogates to the generated gases especially CO. Specifically, the goal of this study is to ensure the suitability of compressed CO_2 to develop a simple process through the intelligent tuning of the advantageous physicochemical properties, which can be helpful to build up a compact system to achieve desired transformation under a mild reaction conditions without any additional components.

Results and discussion

As mentioned before, HMF can undergo different types of reaction, which affect the selectivity of a particular product and eventually require separation step for desired compounds. However, sensitivity of each process strongly depend on the reaction conditions, hence, careful modulation of reaction parameters have utmost importance to shift the reaction path towards the preferred direction. Scheme 1 represents a general transformation routes of HMF. It can be converted to furfuryl alcohol and 2, 5-diformylfuran (DFF) *via* decarbonylation and dehydrogenation, respectively. In addition, DFF can be transformed to furfural again through decarbonylation followed by the hydrogenation to furfuryl alcohol. In addition, dehydrogenation of furfuryl alcohol can produce furfural, which can be decarbonyalted to furan.

Optimisation of different reaction parameters

CO_2 pressure: In the first step of optimisation, selection of proper pressure is essential because of the related tuneable properties of compressed CO_2. To elucidate the effect of CO_2 pressure on the catalytic performance of Pd/Al_2O_3, a series of reactions were performed with the pressure variation from 4 to 16 MPa maintaining the constant temperature (145 °C) and reaction time (4h) in the presence (Figure 1a) and in the absence of air (Figure 1b). As shown in Figure 1a, the reaction proceeds with the change in catalytic activity depending on the applied pressure; very low conversion of ~9% was observed at 4 MPa, which started to increase with the CO_2 pressure and promoted to 38% at 16 MPa. From the product distribution, it can be seen that the selectivity of DFF was comparatively higher (25% at 16 MPa), suggesting

dehydrogenation as another route competing with decarbonylation. Thus, it is reasonable to conduct the reaction in the absence of air to avoid the formation of unwanted by-products.

Figure 1b shows an excellent pressure (density) dependent performance in the absence of air (inert atmosphere). The conversion of HMF was increased significantly even at a low pressure of 4 MPa (79.9%). After reaching a maximum of >99% at 6 MPa, the conversion remain almost constant until 8 MPa. Surprisingly, the conversion of HMF dropped substantially to 54.6%, when the pressure increased to 16 MPa. As CO_2 is a compressed gas, at the fixed temperature of 145 °C, there is a huge change of the density from 0.054 g/ml (vapour) to 0.259 g/ml (supercritical) (NIST chemistry web book) with the increased pressure (4 to 16 MPa), which subsequently affect the solubility of the substrate. Thus, it is reasonable to understand the experimental environment (phase behaviour) inside the reactor, which can provide an explanation on the effect of CO_2 pressure based activity of the present reaction. Because of the technical constrain related to the reactor used to perform the reaction, video monitoring of phase behaviour was conducted in a separate setup. After replicating the applied conditions, it is expected to offer an actual scenario on the number of phases present in the system during the reaction. Figure 2a to 2f show the snapshots taken, while investigating the phase behaviour at various CO_2 pressure. Figure 2a and 2b represent the images of empty cell and after the introduction of HMF, respectively. Naked eye observation indicated a sharp change in the system environment with the alteration of CO_2 pressure (Figure 2c to 2f); at 6 MPa, the view cell is mainly filled up with vapour

and a liquid phase is evident below the stirrer bar (Figure 2c). Interestingly, as the CO_2 pressure enhanced above the 8 MPa, the liquid phase started to decrease (as can be seen from the change in meniscus position) (Figure 2d and 2e), and finally, attained a single phase at 16 MPa. Correlating the phase behaviour with the catalytic activity, it is logical to suggest that adsorption of the substrate on the catalyst surface controlled the reaction, [13] because the substrate is more concentrated around the catalyst when the CO_2 pressure was low and the reaction progressed with accelerated rate. Contrarily, at higher pressure, increased solubility of HMF in compressed CO_2 diluted the substrate concentration near the catalyst surface and generates a HMF enriched CO_2 phase (Scheme 2), which can explain the reduced catalytic performance related to change in the mass transfer properties, affected the catalytic activity.[14]

Effect of temperature: As mentioned before, decarbonylation of aldehyde is an endothermic reaction, hence, most of the literature revealed an exceptionally high temperature regime for catalytic decarbonylation. Conducting the reaction in compressed CO_2, temperature can tuned the density and consequently the solubility, which in turn affect phase behaviour. The conversion of HMF was investigated at the temperature range starting from 80 °C to 150 °C, and a fixed pressure of 6 MPa (Figure 3). Notably, the temperature range studied here maintained the vapour state of CO_2 and there was a nominal change in the density from 0.110 g/ml (80 °C) to 0.0835 g/ ml (145 °C) at the fixed pressure of 6 MPa, thus, no significant change observed in the phase behaviour. The results presented in Figure 3a reveals an unexpectedly poor conversion of HMF (6.1%) at 80 °C, which increased monotonically with temperature and then

level-off at or above 145 °C. Almost quantitative conversion of HMF (>99%) was achieved at 145 °C. There was a significant difference in the product selectivity depending on the temperature; as seen in Figure 3a, the product selectivity transfers from dehydrogenation (DFF) to decarbonylation (FA) at 130 °C; the formation of DFF favoured at low temperature, and continued as the major product from 80 °C (selectivity ~ 80%) to 100 °C (selectivity=61%) (Figure 3a), but decarbonylation dominates above130 °C.

We evaluate the temperature dependent reaction rate corresponds to dehydrogenation (TOF_{DFF}) and decaronylation (TOF_{FA}) in terms of turnover frequency (TOF) at the conversion level of ~6%. Figure 3b shows a comparison between the rate of formation of furfuryl alcohol (TOF_{FA}) and DFF (TOF_{DFF}) related to the applied temperature; at 80 °C, TOF_{FA} (1.6 h^{-1}) was lower than TOF_{DFF} (4.8 h^{-1}), but started to increase with temperature, and reached a maximum of 92.0 h^{-1} at 145 °C. When the temperature further increased to 150 °C, the TOF was slightly improved to 94.1 h^{-1}. On the other hand, except at 80 °C, TOF_{DFF} values are low compared to TOF_{FA} (Figure 3b), and further reduced at higher temperature (12.4 h^{-1}; 145 °C). This suggested that the activation energies of two paths leading to the formation of furfuryl alcohol and DFF are different. Therefore, obtained results underline the importance of applied temperature to dictate the dominance of kinetically or thermodynamically controlled path.[15] Hence, the kinetic reason is a straight forward way to explain the increased TOF_{FA} with temperature rather than correlating the reaction rate with the phase change model as described in Figure 2. From the results presented in Figure 3a and 3b, a

suitable temperature of 145 °C was used as an optimum temperature for HMF decarbonylation.

Reaction time versus catalytic performance: Figure 4a presents the time profile under the applied protocol (temperature=145 ºC and P_{CO2}= 6 MPa). With the variation of reaction time from 15 min. to 8h the activity of the catalyst changed (Figure 4a). There was no detectable transformation right after the introduction of the substrate (0 min.). At the shortest time (15 min.), the conversion of HMF was low (6.1%), but started to increase with time, which reached a maximum of >99% in 4h and then remain almost constant. The change in conversion was also associated with the alteration of the product selectivity; after 15 min., the product mixture contains 76.7% of furfuryl alcohol and DFF (23.3%). No other products were in the detectable range. As the time progressed, the selectivity of furfuryl alcohol increased to 99.6% followed by the reduction of DFF selectivity (0.4%). This observation suggested that the transformation of HMF to furfuryl alcohol can occur (i) *via* direct decarbonylation and (ii) through DFF. The yield *vs.* conversion curve provides further possibility to distinguish between the primary and secondary reaction. The curve with linear approach from the origin represents the primary product, whereas, the product recognised by an increase followed by a decreased yield corresponds to the secondary reaction.[16] The conversion dependent yield plot (Figure 4b) reveals that at the lowest conversion, furfuryl alcohol and DFF obtained with the yield of 3.9% and 1.4%, respectively. Furfuryl alcohol increased steadily with conversion (major path) but DFF disappeared after reaching a maximum (4.4%) at 20% conversion refereeing as a minor path of HMF transformation. Notably, we also detected furfural with a very low yield

(0.6%) at 50% conversion, which, disappeared in the final product. According to the Scheme 1, Furfural can be obtained from the decaronylation of DFF or through the dehydrogenation of furfuryl alcohol. Here, we can ignore the possibility of direct formation from HMF by hydrogenolysis, which require presence of water along with CO_2.[17] In a controlled experiment, DFF was completely converted mainly to furfural (86.3%) (Table 2; Entry 7), on the other hand, experimenting with furfuryl alcohol, although, resulted 36.9%furfural, but with a very poor conversion (5.1 %) (Table 2; Entry 8). Based on the results of controlled experiments, DFF is emerged as a possible source of furfural that can be further hydrogenated to furfuryl alcohol using surface hydrogen also confirmed by another experiment with trace amount of hydrogen (Table 2; Entry 9). Hence, transformation of HMF to furfuryl alcohol can occur through direct decarbonylation (major) as well as *via* DFF (minor) in the present conditions.

Catalyst/substrate ratio: Like other parameters (temperature, pressure etc.), optimisation of catalyst: substrate ratio under the studied reaction conditions is also important. Investigations on the variation of catalyst: substrate (wt.) ratio was carried out from 1:1 to 1:30 at the fixed reaction time of 1h (Figure 5a). At the low ratio of 1:1, complete conversion was observed, but dropped significantly (4.9%) as the substrate amount increased 30 times of the catalyst. After we compare the TOF at the lowest conversion (~ 5%), it shows an enhancement with the increased ratio from 18 h^{-1} (1:1) to 116 h^{-1} (1:30). Thus, ensure to achieve high performance after maximising the substrate concentration, correct use of the reaction conditions are necessary. In this context, lengthening the reaction time could be one of the possibilities to enhance

conversion. Figure 5b presented the catalytic activity and product selectivity after 4h of reaction. Result shows that except 1:1, in which the conversion dropped (70.2%) because of the generation of black polymeric substances, the conversion increased after extending the reaction time to 4h. A highest conversion of >99% was achieved using 1:10 ratio, whereas, a vast improvement (40.2%) was observed for the maximum substrate concentration (1:30). Comparing the product distributions (Figure 5a and 5b), indicated that at the low substrate concentration (1:1), the selectivity of furfuryl alcohol dropped from 93.7% (1h) to 80.2% (4h), which might be attributed to the longer reaction time leads to the substrate scarcity near the catalyst surface and triggered other side reactions. On the other hand, although, higher ratio (1:30) shows improved selectivity of furfuryl alcohol from 52.8% (1h) to 87% (4h), unwanted products (dehydrogenated, condensation etc.) were also detected. Thus, at high substrate concentration, overcrowded surface results increased selectivity of DFF, might be related to the change in adsorption geometry, which influence the activity and selectivity of the reaction.[18] As the time progressed, the transformation of DFF to furfuryl alcohol occurs and the selectivity increased. Hence, in the applied protocol, the catalyst: substrate ratio is a critical parameter to control the activity and selectivity. Targeting maximum conversion and selectivity to furfuryl alcohol, an optimum ratio of 1:10 was used throughout the experiment.

Different organic solvents and solvent-CO_2: After optimisation of the reaction parameters, different organic solvents such as tetrahydrofuran (THF), cyclohexane and hexane were tested for decarbonylation of HMF under the present reaction conditions.

Notably, nonpolar and a borderline (THF) solvents are chosen to compare the activity with compressed CO_2 and the results are shown in Table 1. Applying the same reaction conditions, the conversion of HMF varies depending on the solvent used and follows the order: hexane (92.5%)> cyclohexane (85.2%)> THF (59.1%) (Table 1; Entry 1 to 3). Furfuryl alcohol was detected as the major product independent to the solvent used and the selectivity order is: hexane (95.6%)> cyclohexane (76.9%) > THF (50.1%), showing a clear trend depending on the solvent polarity. No DFF was detected in hexane and cyclohexane (Table 1; Entry 1 and 2), but 43% of DFF enriched product mixture found in THF (Table 1; Entry 3).

After the addition of a fixed pressure of CO_2 (6 MPa) with the above-mentioned solvents a change was observed especially on the selectivity of furfuryl alcohol (Table 1; Entry 4 to 6). The selectivity increased to 90% and 92% in THF and cyclohexane, respectively, (Table 1; Entry 4 and Entry 5) after suppressing the other side reactions observed in the absence of CO_2, however, hexane maintained a constant selectivity (95%). A positive influence was also observed on the conversion of HMF in THF, which increased significantly to 70%, but slightly dropped in the other two solvents. It might be attributed to the presence of co-solvent, which affected the solvation of CO_2 molecule and the activity decreased.[19] Hence, comparing the results with other non-polar solvents it can be infer that compressed CO_2 has decisive influence on the catalytic activity and it is possible to accomplish a significantly improved performance regarding the selectivity of furfuryl alcohol.

Effect of support materials: It has to be mentioned that catalyst support has wide range of effects originates from direct involvement, influencing the particle size (dispersion), charge transfer between metal and support, metal support interaction, redox property etc., which can have lot of consequences to influence the activity.[20] To elucidate the role of support materials on the decarbonylation of HMF in compressed CO_2, we examined Pd, supported on different type of materials (Table 2). In each case, metal concentration was fixed to ~ 0.05 mol%. The dispersion of Pd, calculated from particle size distribution (ESI; Figure S6), which varies from 5% to ~21% depending on the support used. Considering an inert support like MCM-41 (only Si), provides <25% conversion (Table 2; Entry 2), however, after modification with Al, conversion reached to ~ 46% (Table 2; Entry 3). A very high conversion of 86% was observed on Pd/C (Table 2; Entry 4), whereas, 65.2% HMF was converted over Pd/hydrotalcite; a basic support (Table 2; Entry 5). Product distribution also highlights the support effect. In the applied conditions, furfuryl alcohol was the major product on MCM-41 (73.9%) as well as on Al-MCM-41 (90.9%) (Table 1; Entry 2 and 3). In addition, Pd/C also offers an excellent selectivity of furfuryl alcohol (86.6%) accompanied by DFF (10.7%) and 2.7% of other by-products (Table 2; Entry 4). Although, Pd/Al_2O_3 and Pd/hydrotalcite possesses comparable Pd dispersion, dehydrogenation overpowered decarbonylation on hydrotalcite; DFF was obtained as a major product with the selectivity of 58.3% (Table 2; Entry 5). Comparing the conversion and the selectivity of furfuryl alcohol among the catalysts investigated, it follows the order of Al_2O_3> C> hydrotalcite> Al-MCM-41> MCM-41 and Al_2O_3> C> Al-MCM-41> MCM-41> hydrotalcite, respectively. From the results it could be suggested that all the catalysts are

active under the studied condition. Furthermore, the nature of support material plays an important role; acidic supports are more efficient, which can be clarified from their role in the modification of active site (Pd) through the enhancement of electron-deficiency of noble metals compared to the basic supports.[21] The excellent performance of Pd/Al_2O_3 might be related to the possible interaction of Pd with Al_2O_3[22] as Al_2O_3 itself completely inactive for the reaction (Table 2, Entry 6). However, present results do not allow us to reach a precise conclusion, which requires a detail study. Previously, support dependent activity was also observed on the gas phase decarbonylation of furfural.[4]

Scope of the developed method: After a successful application of the developed method on the decarbonylation of HMF, the process was further extended to the other heterocyclic aldehydes at the optimised reaction conditions (temperature=145 °C, reaction time=4h and P_{CO2}=6 MPa) (Table 3). In each case, only decarbonylated product was detected as a sole product. Furfural and 5-methylfurfural were converted to their corresponding decarbonylated compounds with an excellent yield of >99% and 92.5%, respectively (Table 3; Entry 1 and 2). Furthermore, besides the furanic compounds, pyrrole aldehyde was also undergoes decarbonylation to produce pyrrole (yield= 56.2%) (Table 3; Entry 3). The method was then extended on a series of substituted benzaldehyde. Depending on the presence of electron withdrawing and electron donating groups, activity of the compound varies; nitro substituted benzaldehydes are showing good to excellent yield based on the position of the substituent, which follows the sequence of *p*- (100%) > *m*- (90.6%) > *o*- (26.8%) (Table 3; Entry 4, 5 and 6). The presence of –OH and –OMe groups in the *p*-substituted benzaldehyde also affords corresponding decarbonylated products without

affecting the other functional groups; *p*-hydroxybenzaldehyde shows tolerance to –OH group and successfully converted to phenol with 64.4% yield (Table 3; Entry 7). On the other hand, 76% anisole was generated smoothly from the decarbonylation of *p*-anisaldehyde (Table 3; Entry 8). Moreover, 55% toluene was accomplished from *p*-tolylaldehyde (Table 3; Entry 9). Interestingly, styrene reached an excellent yield of 99% from the decarbonylation of *trans*-cinnamaldehyde (Table 3; Entry 10). Indole-3-carbaxaldehyde, a bicyclic compound also decarbonylated to indole with a high yield of 68.3%. Thus, efficiency of the developed method can be confirmed from the powerful performance of a wide range of aldehydes to achieve quantitative selectivity of the targeted decarbonylation products.

Catalyst recycling

Recycling is one of the most claimed advantageous factors of a heterogeneous catalyst considering the environmental and economic sustainability of the process. In the decarbonylation process, it is considered that the catalytic deactivation can be originate from the adsorption of CO on the metal surface. Thus, to check the efficiency of the spent catalyst, it was recycled after separating form the product mixture through filtration (ESI; Figure S1). The used catalyst retained its activity until the 5th recycle and then dropped slightly without affecting the product selectivity. After confirming the stability of the metal by hot filtration test, the surface characterisation of the catalyst was conducted using different spectroscopic techniques.

The transmission electron microscopic (TEM) images of fresh and used catalysts along with their corresponding particle size distributions are shown in Figure 6a and 6b,

respectively. Considering the fresh catalyst, spherical Pd particles of average size 4.2 ± 0.4 nm on Al_2O_3 surface were detected (Figure 6a). Similarly, from the calculation of particle size distributions, TEM image of the spent catalyst (Figure 6b) did not reveal any sign of agglomeration of metal particles or deposition of carbonaceous materials and almost retained the particle size of 4.8 ± 0.3 nm.

The FTIR spectra of fresh and used catalysts were recorded in the range of 4000- 400 cm^{-1} and depicted in Figure S2a and S2b, respectively (details are in the ESI section). In the spectra of the spent catalysts (Figure S2b), there was no peak detected in the 1800-2100 cm^{-1} (dotted rectangle in Figure S2b), assigned to adsorbed CO on metallic Pd,[23] which is one of the possible factors of catalyst deactivation during decarbonylation.[24] High miscibility of CO in compressed CO_2, might prevent the adsorption of CO on the catalyst surface as confirmed from the analysis of gaseous part after the reaction (ESI; Figure S3), eventually improved the catalyst life. Thus, decreased catalytic activity can be related to the loss of catalyst because of handling during separation.

In the fingerprint region (1700-1100 cm^{-1}), FTIR spectra of the used catalyst also shows a number of signals at 1190, 1280, 1400, 1510, 1620 and 1676 cm^{-1} (an expanded view is illustrated in ESI; Figure S4a). The described IR bands belongs to HMF,[25] and the assignments can be made from an overlay spectra of HMF (ESI: Figure S4b; details are in the ESI section). The band at 1676 cm^{-1} is due to the carbonyl group of HMF, which shifted to 1665 cm^{-1} in the used catalyst because of the possible adsorption on Pd, and explain the interaction of HMF with the metal surface through aldehyde functionality.[26] In addition, a very weak band also appears at 1620 cm^{-1}, which might be attributed to the C=C stretching

vibration of furan ring related to the carbonyl group. A small shoulder at 1720 cm^{-1} indicating the possible C=O stretching of aldehyde (marked with *). Regarding the peaks at –OH region (3500-3200 cm^{-1}), the signal became broad compared to the fresh catalyst with a maxima at 3425 cm^{-1} because of the possible change upon adsorption of HMF. In addition, peaks related to the aromatic and aldehyde C-H stretching were also observed at 2920 cm^{-1} and 2860 cm^{-1}, respectively.

To understand the change in the metal environment before and after the reaction, XPS was examined on fresh and recycled catalysts (ESI; Figure S5). Figure S5a and S5b exhibits the 3d region spectra of Pd in fresh and used catalyst, respectively. The Pd 3d core level spectra of the fresh catalyst contains two well separated components corresponding to Pd^0 at 334.9 eV ($3d_{5/2}$) and 340.3 eV ($3d_{3/2}$), which also maintained in the spectra of recycled catalyst (335.3 eV ($3d_{5/2}$) and 340.6 eV ($3d_{3/2}$)). There was no peak related to PdO_x species detected in the higher binding energy region. The atom concentration calculated in the fresh and recycled catalyst are 4.7% (Pd), 36.8% (Al), 58.5% (O) and 4.4% (Pd), 37.2% (Al), 58.7% (O), respectively. In addition, XPS revealed a slight changes in the amount of Pd atoms on the surface of Pd/Al_2O_3 measured in terms of Pd/Al ratio, which has been increased slightly from the fresh catalyst (0.072) to the recycled one (0.110) attributing a nominal change in dispersion of the metal on catalyst surface.[27] The XPS spectra of the support materials confirmed a minor changes in the binding energies of Al2p and O1s spectra (ESI).

Possible mechanism

Elucidation of reaction mechanism is important to understand the each reaction steps and helpful for further implementation of the developed method. It is difficult to predict a clear

cut mechanism for the studied reaction, based on the present results, thus, an outline can be proposed (Scheme 3). In the present system, the reaction was conducted in compressed CO_2, and there is every possibility of the chemical participation of CO_2 [28] through the direct interaction with the substrate [29] and with the catalyst.[30] Considering the experimental results, we observed that the highest catalytic activity obtained in the substrate-rich phase, hence, cancelling the possibility of substrate-CO_2 interaction. The IR spectra of the used catalyst shows no bands related to the carbonate species generally occurred in the presence of CO_2 [31]. Therefore, in the present system, CO_2 can be considered as a CO acceptor, which causes a shift in the reaction equilibrium and enhanced the reaction rate (ESI; Figure S3).

The best performance of the catalyst was achieved in the two phase condition (CO_2-substrate), suggesting a surface controlled reaction, but only support surface (Al_2O_3) is completely inactive for the reaction, which require Pd (Table 2; Entry 6). Therefore, considering the entire scenario, we proposed that in the first step, HMF invariably adsorbed on the metal surface through the aldehyde functionality as confirmed from the product distribution. From the spectral analysis of the used catalysts, we also detected a shifting of the aldehyde -C-O band and a change in the aromatic skeletal vibration region (1600 and 1500 cm^{-1}). The transformation of HMF into furfuryl alcohol can be postulated as the consequence of the C-C bond scission between the aryl and aldehyde group. Previously, Song *et al.* reported that the cleavage of C-C bond is easier than C-H bond for aryl aldehyde due to the strong interaction between the aryl group and the catalyst surface, which causes weakening of the C-C bond.[32] In addition, a strong interaction of aldehyde group and furan ring with the same metal surface was also reported.[33] In the next step,

cleavage of the C-C bond causes decarbonylation followed by reductive elimination and results the decarbonylated product. The minor reaction path of dehydrogenation might be the consequence of the interaction of -OH proton with neighbouring surface oxygen.[34] Furthermore, the role of the support material cannot be ignored as described in the previous section, which needs further investigations.

Conclusion

In conclusion, we have developed an efficient decarbonylation methodology free from any organic solvent or any CO scavenger for the selective decarbonylation of biomass-based platform molecule like HMF using a commercially available Pd/Al_2O_3 catalyst in compressed CO_2. The unique properties of the reaction medium can be applied beneficially in the conversion of HMF to furfuryl alcohol with very high selectivity (99.6%). Indeed, the incorporation of compressed CO_2 significantly improved the catalytic activity. Neither CO_2, nor Pd alone appear as suitable for the reaction, but a combination of both provides high catalytic performance and excellent product yield through the proper control of the reaction variables. A minor path through dehydrogenation was also detected, but has nominal effect on the product selectivity. This process allows an easy separation of product simply by depressurisation. Based on the characterisation of the fresh and used catalyst, a reaction mechanism was proposed. The catalytic system provides appreciable reusability and shows tolerance to a series of different types of substrates with various substituents, which generate corresponding decarbonylated compounds with good to excellent yield without affecting the substituent present. Our future challenge is to investigate the role of

oxide support in the presence of compressed CO_2 and to determine the exact reaction mechanism after the proper understanding of status of the reaction medium.

Experimental

Materials: 5-hydroxymethylfurfural (HMF) (Aldrich) was used as received. Carbon dioxide (>99.99%) was supplied by Nippon Sanso Co. Ltd. 5% Pd/C, 5% and 1 %Pd/Al_2O_3, were from Aldrich. Pd (II) sodium chloride from Aldrich. ~ 1% Pd/hydrotalcite from Wako Pure Chemicals. Cetyltrimethylammonium bromide used as template for MCM-41 synthesis was from Aldrich. Tetraethylorthosilicate, which was used as silica source from Wako Pure Chemicals.

Metal catalysts supported on MCM-41 was synthesised in our laboratory using a modified method.[35] In each case, metal content was maintained as ~5 %. Unless otherwise stated all the chemicals were used without any further purifications. Detail of catalyst characterisation techniques are in the ESI section.

Phase observation: Video monitoring of the phase behaviour of HMF in compressed CO_2 at 145 °C was studied separately in a 10 ml high pressure view cell. At first, HMF was introduced into the cell followed by the introduction of CO_2 after the stabilisation of temperature. For phase observation during the reaction, the content was stirred continuously and in each step, images were recorded.

Catalytic performance: A 50 ml batch reactor placed in a hot air circulating oven was used for testing the reaction in laboratory scale. In a typical experiment, a specified amount of the catalyst and substrate were introduced into the reactor. Notably, the

reactor was flushed 5 times with nitrogen to remove air. The reactor was heated for a specified amount of time to stabilise to the required temperature (145 °C). After stabilisation, CO_2 was charged into the reactor using a high-pressure liquid pump and then compressed to the desired pressure. The content of the reactor was stirred with a magnetic stirrer bar during the reaction. The reactor was quenched using an ice bath after the reaction, followed by a careful depressurisation and the separation of solid catalyst from liquid product simply by filtration. Detailed analytical method is given in the ESI section.

Acknowledgements

H. K. is funded by the Japan-U.S. cooperation project for research and standardization of Clean Energy Technologies, The Ministry of Economy, Trade and Industry (METI), Japan and CREST, Japan Science and Technology (JST).

References

1. *a)* J. Tsuji, *J. Am. Chem. Soc.* 1968, **90**, 99; *(b)* D. H. Doughty and L. H. Pignolet, *J. Am. Chem. Soc.* 1978, **100**, 7083; *(c)* J. M. O'Connor and J. Ma, *J. Org. Chem.* 1992, **57**, 5075; *(d)* P. Fristrup, M. Kreis, A. Palmelund, P.-O. Norrby and R. Madsen, *J. Am. Chem. Soc.* 2008, **130**, 5206; (e) J. J. Adams, N. Arulsamy and D. M. Roddick, *Organometallics* 2012, **31**, 1439; *(f)* T. Iwai, T. Fujihara and Y. Tsuji, *Chem. Commun.* 2008, 6215.
2. *(a)* A. Modak, A. Deb, T. Patra, S. Rana, S. Maity and D. Maiti, *Chem. Commun.* 2012, **48**, 4253; *(b)* K. Ding, S. Xu, R. Alotaibi, K. Paudel, E. W. Reinheimer and J. Weatherly, *J. Org. Chem.* 2017, **82**, 4924.
3. *(a)* M. Kreis, A. Palmelund, L. Bunch and R. Madsen, *Adv. Synth. Catal.* 2006, **348**, 2148; *(b)* C. M. Beck, S. E. Rathmill, Y. J. Park, J. Chen, R. H. Crabtree, L. M. Liable-Sands and A. L. Rheingold, *Organometallics* 1999, **18**, 5311.
4. *(a)* H. Singh and M. P. P. D. Srivastava, *J. Chem. Tech. Biotech.* 1980, **30**, 293; *(b)* P. Lejemble and A. Gaset, P. Kalck *Biomass,* 1984, **4**, 263.
5. *(a)* P. K. Kundu, M. Dhiman, A. Modak, A. Chowdhury, V. Polshettiwar and D. Maiti *ChemPlusChem* 2016, **81**, 1142; *(b)* V. V. Pushkarev, N. Musselwhite, K. An, S. Alayoglu and G. A. Somorjai, *Nano Lett.* 2012, **12**, 5196; *(c)* N. Pino, S. Sitthisa, Q. Tan, T. Souza, D. López and D. E. Resasco, *J. Catal.* 2017, **350**, 30.
6. *(a)* A. Corma, S. Iborra and A. Velty, *Chem. Rev.* 2007, **107**, 2411; *(b)* O. Casanova, S. Iborra and A. Corma, *ChemSusChem* 2009, **2**, 1138; *(c)* Y. Roman-Leshkov, J. N. Chheda, and J. A. Dumesic, *Science* 2006, **312**, 1933; *(d)* H. B.

Zhao, J. E. Holladay, H. Brown and Z. C. Zhang, *Science* 2007, **316**, 1597; *(e)* G. Yong, Y. G. Zhang and J. Y. Ying, *Angew. Chem.* 2008, **120**, 9485; *Angew. Chem. Int. Ed.* 2008, **47**, 9345; *(f)* L. Vanoye, M. Fanselow, J. D. Holbrey, M. P. Atkins and K. R. Seddon, *Green Chem.* 2009, **11**, 390; *(g)* S. Hu, Z. Zhang, J. Song, Y. Zhou and B. Han, *Green Chem.* 2009, **11**, 1746; *(h)* J. Lewkowski, ARKIVOC 2001, **2**, 17.

7. *(a)* G. Tsilomelekis, M. J. Orella, Z. Lin, Z. Cheng, W. Zheng, V. Nikolakis and D. G. Vlachos, *Green Chem.* 2016, **18**, 1983; *(b)* A. Herbst and C. Janiak *New J. Chem.,* 2016, **40**, 7958; *(c)* B. Girisuta, M. B. P. L. Janssen and J. H. A. Heeres, *Green Chem.* 2006, **8**, 701.
8. J. Mitra, X. Zhou and T. Rauchfuss, *Green Chem.*, 2015, **17**, 307.
9. Y.-B. Huang, Z. Yang, M.-Y. Chen, J.-J. Dai, Q.-X. Guo, and Y. Fu, *ChemSusChem* 2013, **6**, 1348.
10. *(a)* Q. Meng, C. Qiu, G. Ding, J. Cui, Y. Zhu and Y. Li *Catal. Sci. Technol.*, 2016, **6**, 4377; *(b)* Q. Meng, D. Cao G. Zhao, C. Qiu, X. Liu, X. Wen, Y. Zhu and Y. Li, *Appl. Catal. B: Environmental* 2017, **212**, 15.
11. F. M. A. Geilen, T. vom Stein, B. Engendahl, S. Winterle, M. A. Liauw, J. Klankermayer, and W. Leitner. *Angew. Chem. Int. Ed.* 2011, **50**, 6831.
12. M. Chatterjee, T. Ishizaka, A. Chatterjee and H. Kawanami, *Green Chem.*, 2017, **19**, 1315.

13. *(a)* A. Milewska, A. M. Banet Osuna, I. M. Fonseca and M. Nunes da Ponte, *Green Chem.*, 2005, **7**, 726; *(b)* D. Chouchi, D. Gourgouillon, M. Courel, J. Vital and M. Nunes da Ponte, *Ind. Eng. Chem.Res.*, 2001, **40**, 2551.

14. N. J. Meehan, A. J. Sandee, J. N. H. Reek, P. C. J. Kamer, P.W. N. M. van Leeuwen and M. Poliakoff, *Chem. Commun.*, 2000, 1497.

15. P. Sykes, A guidebook to mechanism in organic chemistry, 6th ed., Longman Scientific & Technical, Essex, UK, 1986, pp. 42–43.

16. A.-N. Ko and B. Wojciechowski, *Prog. Reaction Kinetics* 1983, **12**, 20.

17. M. Chatterjee, T. Ishizaka and H. Kawanami *Green Chem.* 2014, **16**, 1543.

18. *(a)* F. Delbecq and P. Sautet, *J. Catal.* 1995, **152**, 217; *(b)* D. Loffreda, F. Delbecq, F. Vigné, and P. Sautet *J. Am. Chem. Soc.*, 2006, **128**, 1316.

19. *(a)* T. Aizawa, S. Janttarakeeree, Y. Ikushima, N. Saitoh, K. Arai and R. Smith, *J. Supercrit. Fluids* 2003, **27**, 247; *(b)* A. I. Frolov and M. G. Kiselev *J. Phys. Chem. B* 2014, **118**, 11769.

20. *(a)* T. Ishihara, K. Harada, K. Eguchi and H. Arai, *J. Catal.* 1992, **136**, 161; *(b)* M. Shekhar, J. Wang, W.-S. Lee, W. D. Williams, S. M. Kim, E. A. Stach, J. T. Miller, W. N. Delgass, and F. H. Ribeiro, *J. Am. Chem. Soc.* 2012, **134**, 4700.

21. *(a)* A. Yu. Stakheev, L. M. Kustov, *Appl. Catal. A: General* 1999, **188**, 3; *(b)* R. A, Della Betta, M. Boudart, P. Gallezot and R. S. Weber, *J. Catal.* 1981, **69**, 514.

22. *(a)* J. H. Kwak, J. Z. Hu, D. H. Mei, C. W. Yi, D. H. Kim, C. H. F. Peden, L. F. Allard and J. Szanyi, *Science* 2009, **325**, 1670; *(b)* D. H. Mei, J. H. Kwak, J. Z.

Hu, S. J. Cho, J. Szanyi, L. F. Allard and C. H. F. Peden, *J. Phys. Chem. Lett.* 2010, **1**, 2688.

23. *(a)* F. M. Hoffmann, *Surf. Sci. Rep.* 1983, **3**, 107; *(b)* C. Keresszegi, T. Burgi, T. Mallat and A. Baiker, *J. Catal.* 2002, **211**, 244.
24. *(a)* R. D. Srivastava and A. K. Guha, *J. Catal.* 1985, **91**, 254; *(b)* M. D. Argyle and C. H. Bartholomew, *Catalysts* 2015, **5**, 145.
25. N. B. Colthup, L H. Daly and S. E. Wiberley Introduction to Infrared and Raman Spectroscopy New York: Academic Press
26. H.-W. Chen, C.-S. Chen, and S.-J. Ham, *J. Phys. Chem.* 1995, **99**, 10557.
27. B. Kucharczyk, W. Tylus and L. Kepinski, *Appl. Catal. B: Environmental* 2004, **49**, 27.
28. M. A. Blatchford, P. Raveendran and S. L. Wallen, *J. Am. Chem. Soc.* 2002, **124**, 14818.
29. Y. Jing, Y. Hou, W. Wu, W. Liu, and B. Zhang, *J. Chem. Eng. Data* 2011, **56**, 298.
30. *(a)* J. Szanyi and J. H. Kwak, *Phys. Chem. Chem. Phys.*, 2014, **16**, 15126; *(b)* K. Fottinger, R. Schlogl and G. Rupprechter, *Chem. Commun.* 2008, 320.
31. X. Wang, H. Shi, J. H. Kwak and J. Szanyi, *ACS Catal.* 2015, **5**, 6337.
32. R. Song, D. Ostgard and C. V. Smith, in Catalysis of organic reactions Edited by , J. L. Davis and M. A. Barteau, *Surf. Sci.* 1987, **187**, 387.
33. *(a)* S. Sitthisa, T. Pham, T. Prasomsri, T. Sooknoi, R. G. Mallinson and D. E. Resasco, *J. Catal.* 2011, **280**, 17; *(b)* S. H. Pang and J. Will Medlin, *ACS Catal.* 2011, **1**, 1272.

34. *(a)* L. Nondek and J. Sedlacek, *J. Catal.* 1975, **40**, 34; *(b)* B. Xu, X. Liu, J. Haubrich and C. M. Friend, *Nat. Chem.* 2010, **2**, **61.**

35. M. Chatterjee, T. Iwasaki, Y. Onodera and T. Nagase *Catal. Lett.* 1999, **61**, 199.

Legend to figures

Figure 1. Effect of CO_2 pressure on the decarbonylation of HMF using Pd/Al_2O_3 catalyst; (a) Presence of air and (b) N_2 atmosphere. Reaction conditions: Catalyst: substrate= 1:10; temperature= 145 ºC and reaction time= 4 h.

Figure 2: Images taken during phase observation of HMF-CO_2 system in a view cell at 145 °C. (a) Empty, (b) HMF in cell at various CO_2 pressure (c) 6 MPa, (d) 8 MPa, (e) 12 MPa and (e) 16 MPa. For 12 and 16 MPa, snapshot taken during stirring is presented, which clearly shows the status of HMF. Dotted red line represents the liquid meniscus.

Figure 3: Temperature effect on the (a) catalytic activity and selectivity and the rate of (b) decarbonylation (TOF_{FA}) and dehydrogenation (TOF_{DFF}) over Pd/Al_2O_3 catalyst. Reaction conditions: Catalyst: substrate= 1:10; P_{CO2} = 6 MPa and reaction time= 4h. TOF= Turnover frequency (TOF) = number of moles reacted/ moles of metal x time (calculated on the basis of lowest conversion of around 6 %).

Figure 4: Time profile of the (a) catalytic decarbonylation of HMF and (b) yield *vs.* conversion on Pd/Al_2O_3 catalyst. Reaction conditions: Catalyst: substrate= 1:10; P_{CO2} = 6 MPa and temperature = 145 ºC.

Figure 5: Effect of catalyst: substrate ratio (wt.) on the activity of Pd/Al_2O_3 catalyst at (a) 1h and (b) 4h. Reaction conditions: P_{CO2} = 6 MPa and temperature= 145 ºC.

Figure 6: TEM images along with particle size distribution of the Pd/Al_2O_3 catalyst: (a) fresh and (b) used.

Scheme 1: A general reaction pathway of HMF transformation.

Scheme 2: Pictorial representation of possible scenario inside the reactor at (a) low and (b) high pressure conditions.

Scheme 3: Proposed reaction mechanism.

Table 1: Decarbonylation of HMF in different organic solvents and in solvent+CO_2 using Pd/Al_2O_3 catalyst.

Entry	Solvent	Conv. (%)	Product selectivity (%)			
			Furfuryl alc.	DFF	Furfural	Others
Organic solvent						
1	THF	59.1	60.1	32.9	6.9	-
2	Cyclohexane	85.2	76.9	-	5.2	17.9
3	Hexane	92.5	95.6	-	4.4	-
Organic solvent + CO_2						
4	THF	70.0	90.9	5.5	3.3	-
5	Cyclohexane	81.4	92.0	3.4	4.6	-
6	Hexane	84.0	95.5	-	4.5	=

Reaction conditions: catalyst: substrate=1:10; P_{N2}= 0.1 MPa; Temp. =145 °C; reaction time= 4h; metal content ~ 5 wt. %; Entries 1-3: solvent= (~ 7 ml corresponds to the moles of CO_2 used); Entries 4-6: P_{CO2}= 6 MPa.

Table 2: Activity of supported Pd catalysts for decarbonylation of HMF in compressed CO_2

Entry	Catalyst	Dispersion [a] (%)	Conv. (%)	Product selectivity (%)		
				DFF	Furfuryl alc.	Other
1	Pd/Al_2O_3	21.4	99.8	0.4	99.6	-
2	Pd/MCM-41	5.6	22.8	26.1	73.9	-
3	Pd/Al-MCM-41	4.8	45.6	9.1	90.9	-
4	Pd/C	12.1	86.0	10.4	86.6	2.7
5	Pd/Hydrotalcite	20.2	65.2	58.3	37.9	3.8
6	Al_2O_3	-	-	-	-	-
7[b]	Pd/Al_2O_3	-	>99.0	-	-	>99.0[c]
8[d]	Pd/Al_2O_3	-	5.1	-	-	>99.0[e]
9[f]	Pd/Al_2O_3		>99.0	-	97.8	-

Reaction condition: catalyst: substrate=1:10; P_{CO2}= 6 MPa; P_{N2}= 0.1MPa; Temp. =145 °C; reaction time=4h; 0.05 mol% of Pd. [a] approximate expression of metal dispersion = 0.9/diameter (in nm); [Ref.: M. Boudart, G. Djega-Mariadassou, *Kinetics of Heterogeneous Catalytic Reaction*; Princeton University Press: Princeton, NJ, 1984]; [b] DFF as substrate, [c] 86.3 %= furfural and 13.7 %= other; [d] furfuryl alcohol as substrate; [e]36.9 % furfural and 63.1 % condensation products; [f] controlled experiment with DFF in the presence of trace amount of hydrogen for 1h.

Table 3: Substrate scope of decarbonylation reaction on Pd/Al_2O_3 catalyst

Entry	Substrate	Product Yield (%)
1[a]	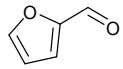	 (>99.0)
2	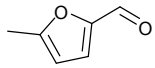	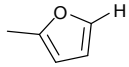 (92.5)
3	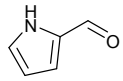	 (56.2)
4	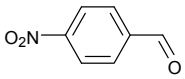	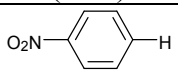 (>99.0)
5	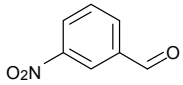	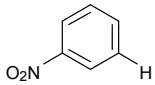 (90.6)
6	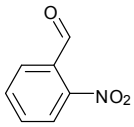	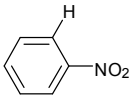 (26.8)
7	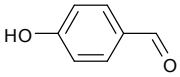	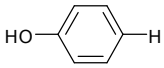 (64.4)
8	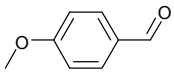	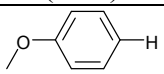 (75.8)
9	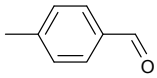	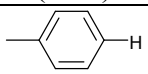 (53.7)
10	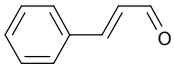	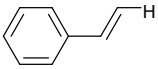 (98.9)
11[b]	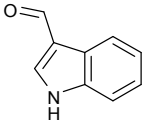	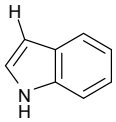 (68.3)

Reaction conditions: catalyst: substrate=1:10; P_{CO2}= 6 MPa; P_{N2}= 0.1MPa; Temp. =145 °C; time= 4h. a= 6.5h, b= 12h; in each case, decarbonylated product was detected as the sole product.

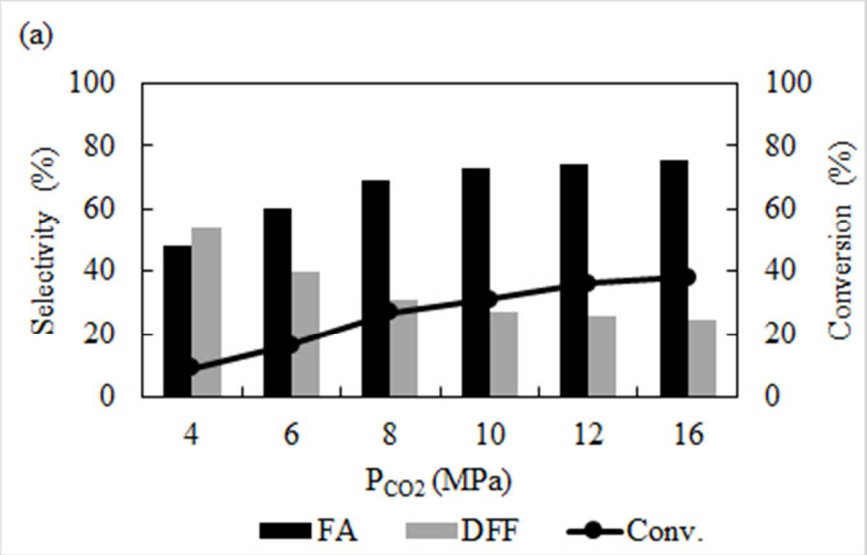

152x98mm (72 x 72 DPI)

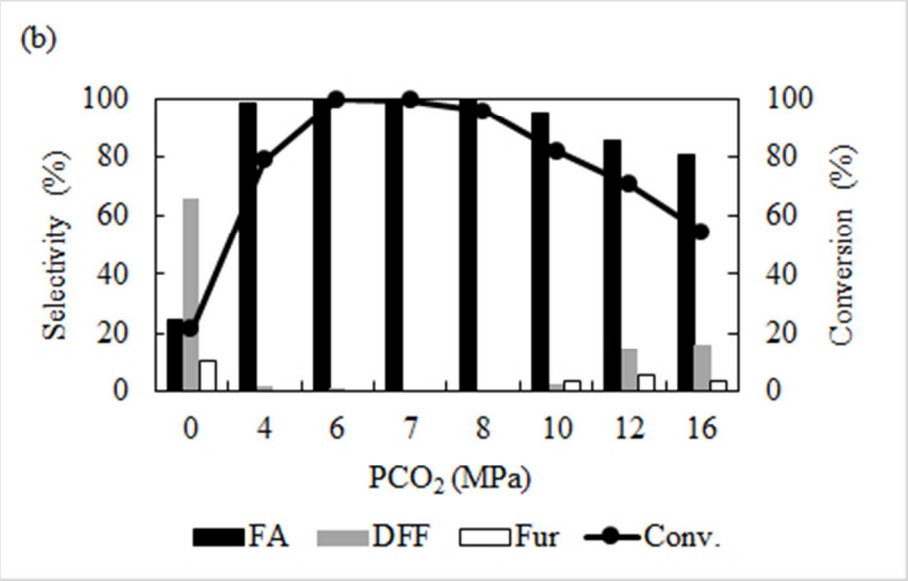

160x102mm (72 x 72 DPI)

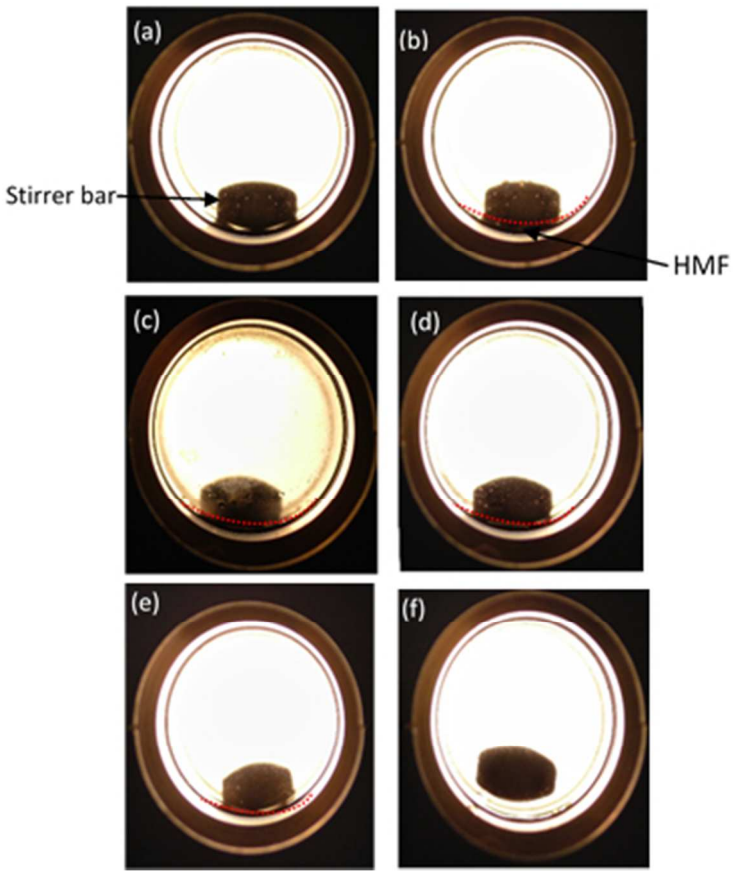

136x152mm (72 x 72 DPI)

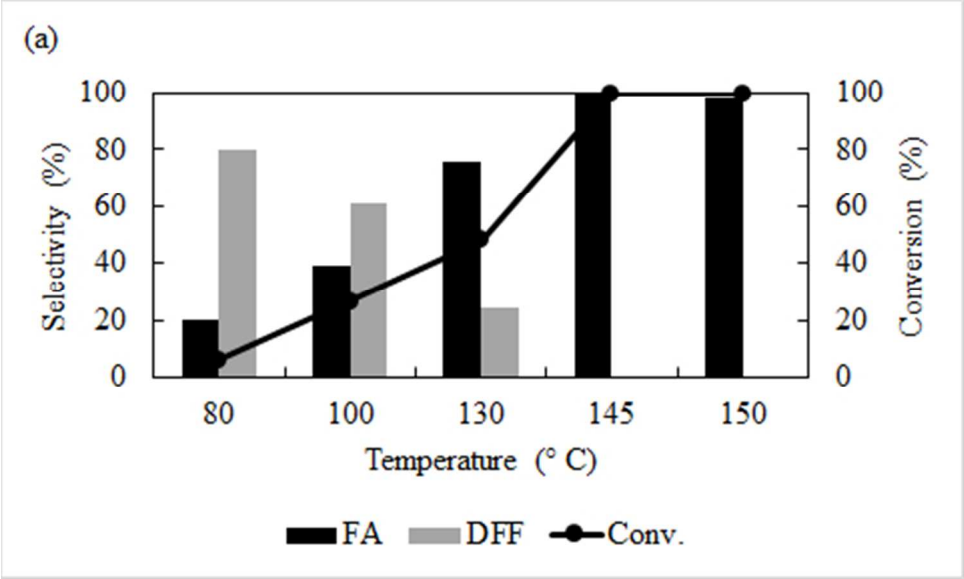

169x101mm (72 x 72 DPI)

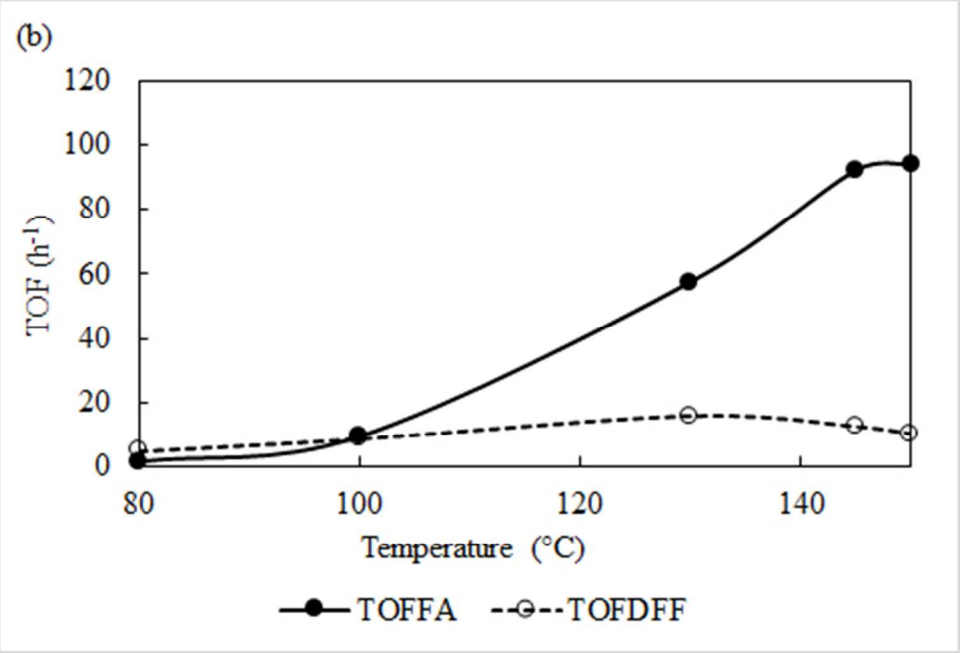

169x115mm (72 x 72 DPI)

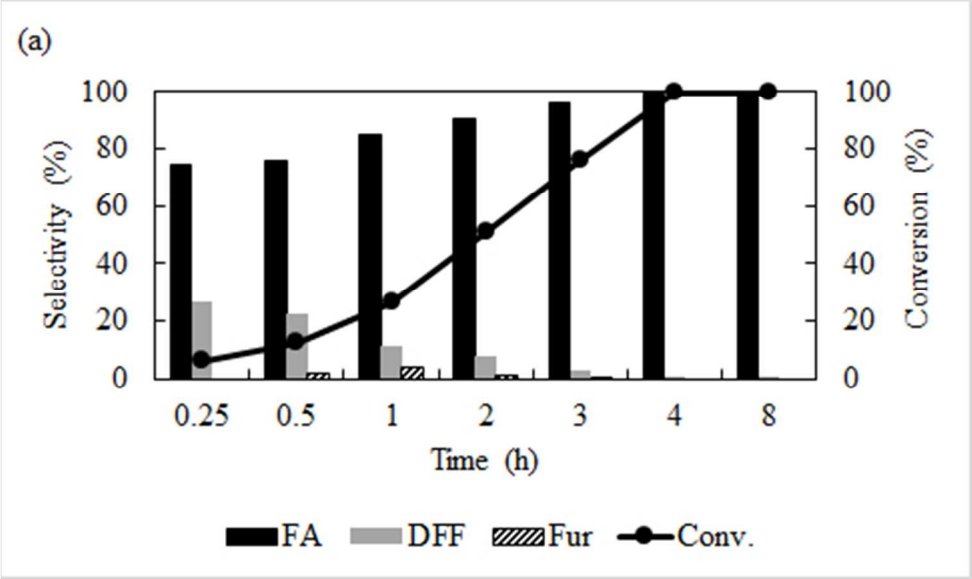

171x101mm (72 x 72 DPI)

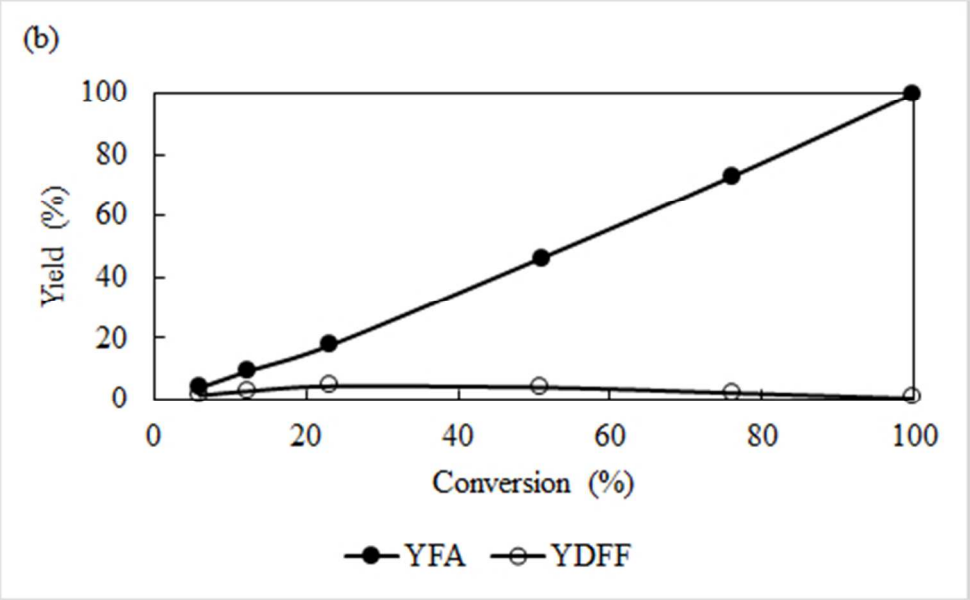

170x105mm (72 x 72 DPI)

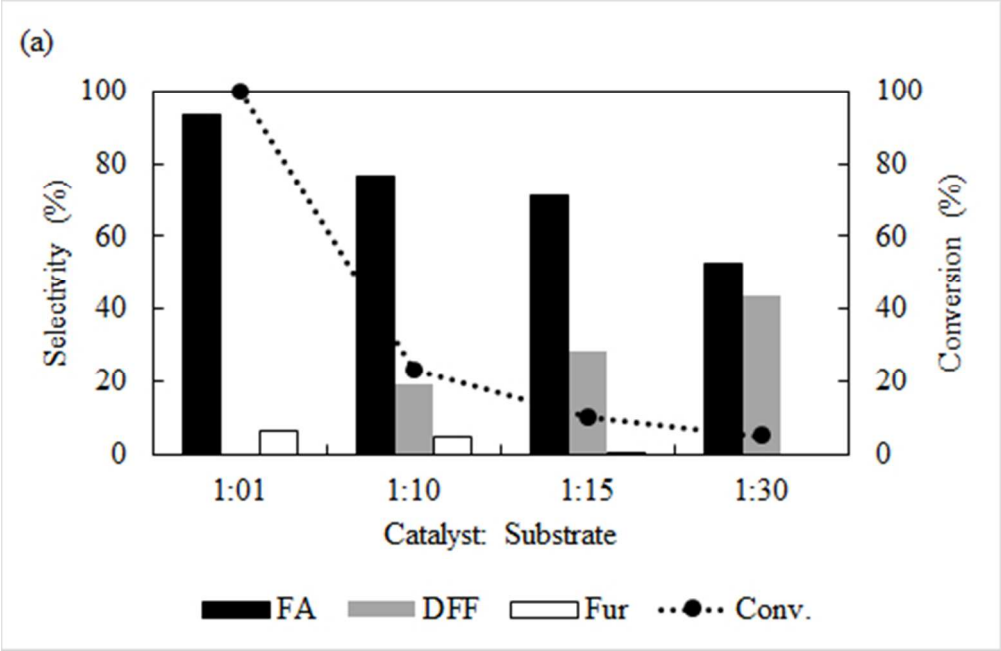

178x116mm (72 x 72 DPI)

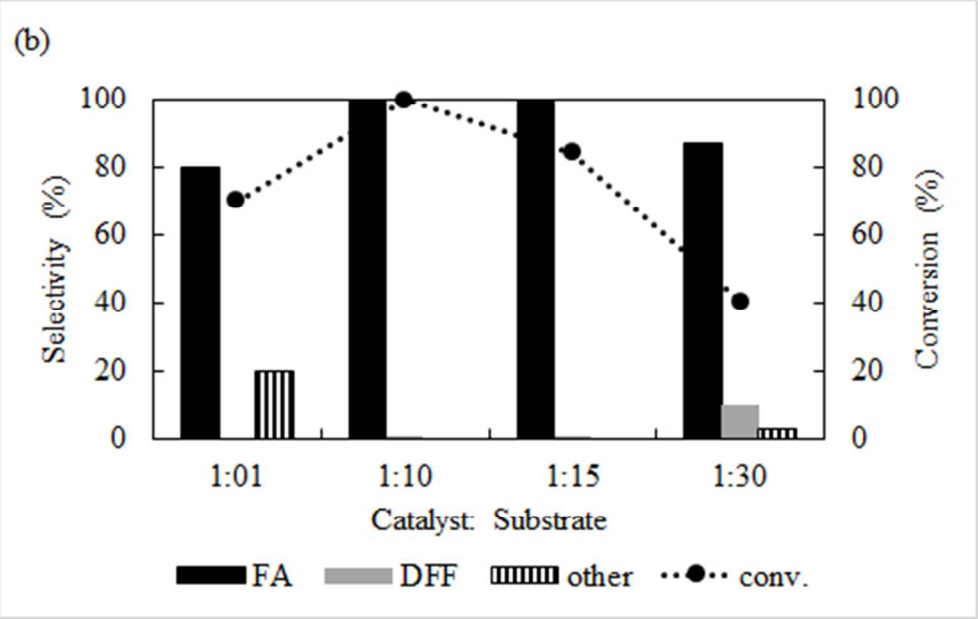

172x109mm (72 x 72 DPI)

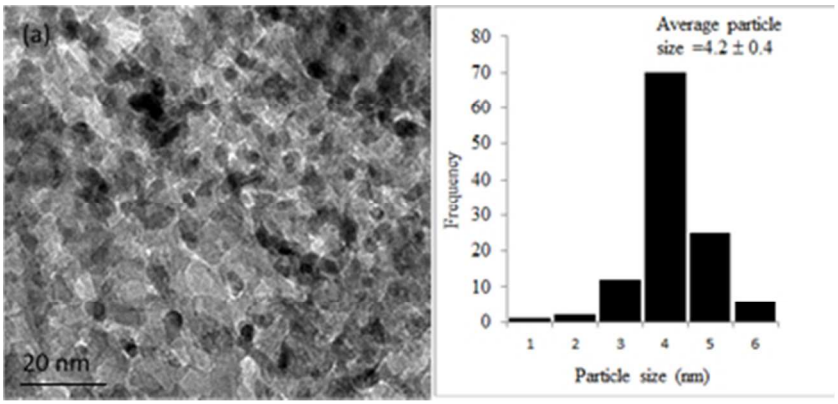

146x69mm (72 x 72 DPI)

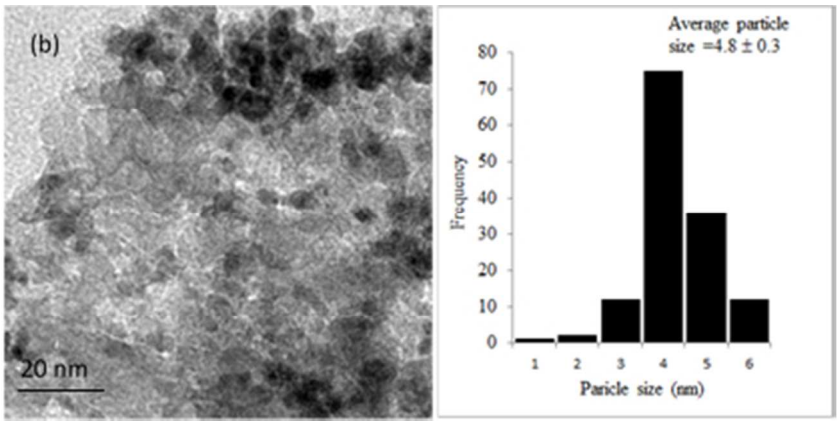

147x73mm (72 x 72 DPI)

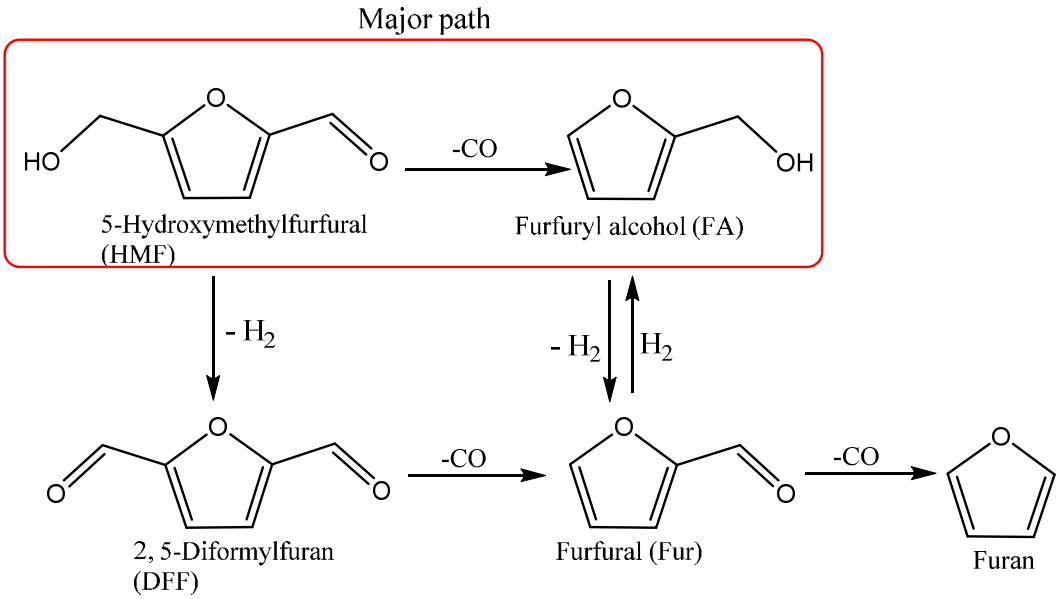
Major path
HO
O
O
-CO
O
OH
5-Hydroxymethylfurfural
(HMF)
Furfuryl alcohol (FA)
- H2
- H2
H2
O
O
-CO
O
O
-CO
O
2, 5-Diformylfuran
(DFF)
Furfural (Fur)
Furan

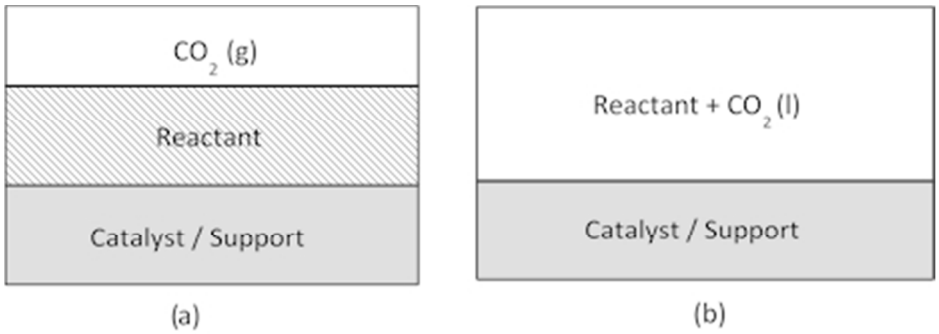

164x60mm (72 x 72 DPI)

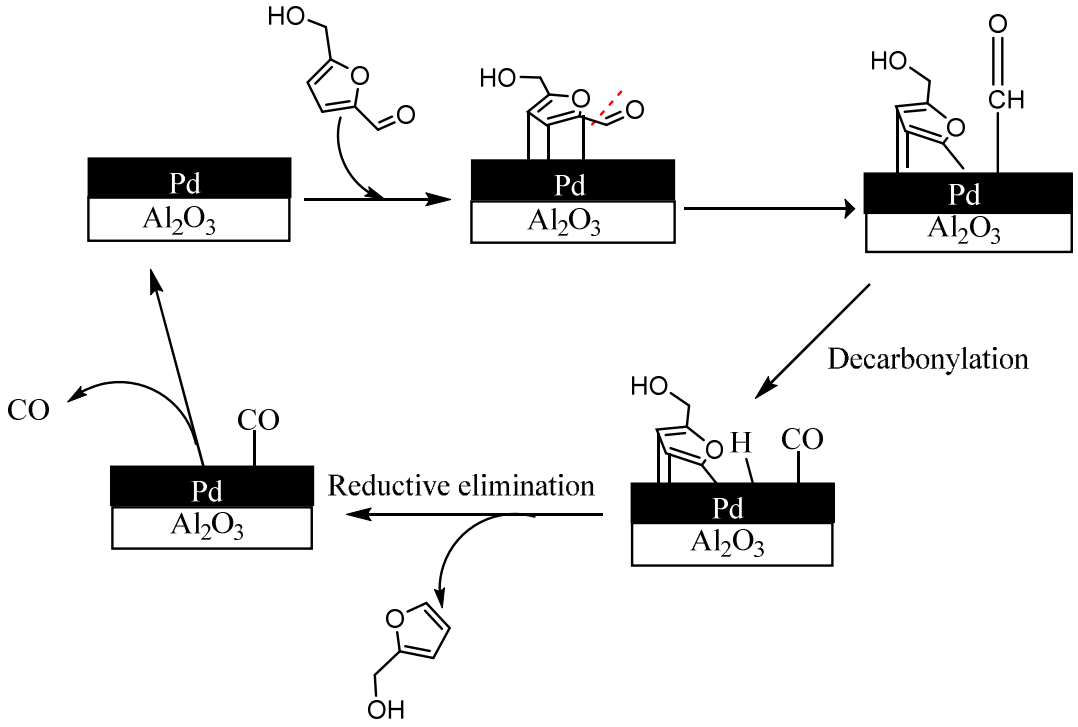
HO
O
O
Pd
Al2O3
HO
O
O
Pd
Al2O3
O
HO
CH
O
Pd
Al2O3
Decarbonylation
HO
O
H
CO
Pd
Al2O3
Reductive elimination
CO
CO
Pd
Al2O3
O
OH

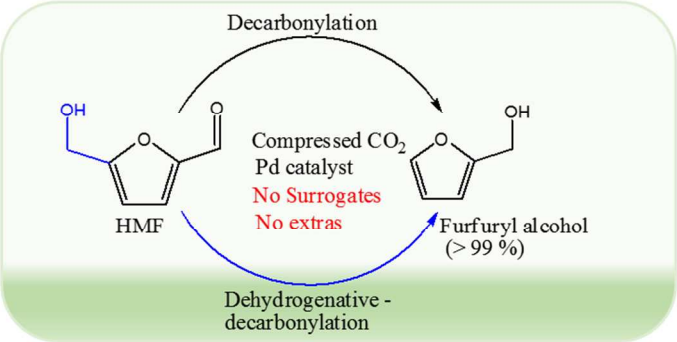

The high efficiency of compressed CO_2 in combination with metal catalyst was unfold on the decarbonylation of HMF successfully.